Hindawi
Advances in Meteorology
Volume 2022, Article ID 9183882, 14 pages
https://doi.org/10.1155/2022/9183882

Research Article

Spatiotemporal Climate Variation and Analysis of Dry-Wet Trends for 1960–2019 in Jiangsu Province, Southeastern China

Mengsheng Qin,[1] **Liting Zhang**,[1] **Shiquan Wan**,[1] **Yuan Yue**,[2] **Qiong Wu**,[1] **and Lu Xia**[1]

[1]*Yangzhou Municipal Meteorological Bureau, Yangzhou, China*
[2]*Jilin Meteorological Bureau, Changchun, China*

Correspondence should be addressed to Shiquan Wan; wan_sq@qq.com

Received 6 May 2022; Accepted 5 August 2022; Published 27 August 2022

Academic Editor: Upaka Rathnayake

The spatiotemporal characteristics of dry-wet trends were identified and assessed, and the dominant meteorological factors were identified for the climate of Jiangsu province in humid southeastern China for the period 1960–2019. We conducted the research using data for the entire Jiangsu province as well as three major regions in Jiangsu (Huaibei, Jianghuai, and Sunan) with different regional climates. The results showed that decreased precipitation and relative humidity in spring and autumn over the study period were mainly responsible for the dry trends of the climates of all three regions and the entire province. Precipitation had a greater influence in spring and relative humidity in autumn. Decreases in sunshine hours and wind speed were responsible for the summer wet trends of the climates of Huaibei and Jianghuai and the entire province. However, precipitation increased significantly in the summer and was responsible for the increasing wet trend in Sunan. Significantly increased precipitation in winter was primarily responsible for the increasing wetness in Jianghuai and Sunan and the entire province in that season. However, the wet trend in northern Huaibei in winter was mainly caused by the decrease in wind speed over the study period. For the growing season and annually, the positive effects of changes in wind speed, sunshine hours, and precipitation led to increased humidity index in Jianghuai, Sunan, and the entire province. Precipitation showed a decreasing trend that countered the positive effects of decreases in wind speed and sunshine hours, which resulted in a slight decrease in the humidity index in Huaibei for both the growing season and annually. Sensitivity analysis indicated that the humidity index was positively sensitive to precipitation and relative humidity and negatively sensitive to air temperature, wind speed, and sunshine hours in Jiangsu province during 1960–2019. Overall, the humidity index in this region of southeastern China was most sensitive to changes in precipitation followed, in order of sensitivity, by sunshine hours, air temperature, wind speed, and relative humidity. Our findings provide a theoretical basis for adjusting irrigation programs and efficient utilization of water resources at the regional scale in humid southeastern China.

1. Introduction

It is well recognized that extreme weather events are largely caused by global climate change and anthropogenic activity [1], and they severely affect human society and the natural environment [2]. Drought is a significant and influential meteorological phenomenon in most climate zones [3]. Widespread drought causes tremendous economic losses and is a great threat to food, water and energy security, civil society, and natural habitats [2, 4–6]. It is therefore important to study the spatiotemporal characteristics of droughts and their causes; that is, to analyze and predict spatiotemporal variations in indicators of extreme wet or dry conditions and to identify reasons for these variations.

Researchers have developed dry and wet indexes based on air temperature (T_a), wind speed (WS), precipitation (Pre), reference evapotranspiration (ET_o), and other meteorological factors [7]. These indexes include the Palmer drought severity index (PDSI) [8], the standardized precipitation index (SPI) [9], the humidity index (HI) [10], and the standardized precipitation evapotranspiration index (SPEI) [11, 12]. Yang et al. [13] compared the applicability of

these indicators to China's conditions and recommended that the HI be used in this country. Ma and Fu [14] found that HI had performed well in China over the last five decades. HI, which reflects changes in precipitation and air temperature, has been used extensively in studies around the world [15–20].

In the literature review, it is found that the variations in dry-wet trends and their causes have been examined for different seasons, regions, and durations worldwide. Chinese researchers have studied the annual increase in aridity in regions within China such as the Zoige Wetland [21], Bosten Lake [22], Loess Plateau [15], semi-arid or semi-humid areas [6], the entire northern part of China [23], and even China in its entirety [7]. Annual dry trends have been identified in other countries such as Korea [24], Iran [16], Guatemala [25], Iraq [20], Rwanda [26], India [27], Middle East [28], and Iberian Peninsula [29]. In general, these studies attributed the drying mainly to surface warming, decreased precipitation, and increased evapotranspiration [5–7, 15, 16, 20, 21, 27–29]. However, the main drivers of the wet trends in the Yangtze River Delta in eastern China [1] and the Tibetan Plateau, North Xinjiang, and the Tuotuo River of western China [30–32], were found to be increased precipitation and relative humidity (RH) together with a reduction in wind speed and sunshine hours (SSH) [1, 30–32]. It was also observed that the dominant meteorological variables caused opposite dry-wet trends in different months or seasons. For example, Jin et al. [21] found that the Zoige Wetland in southwestern China tended to become drier in spring and winter and wetter in summer and autumn during the period 1961–2016. In the Zhejiang province of southeastern China, in the period 1971–2015, there were dry trends in April, May, and September, a wet trend in August, and no observable dry or wet trends in other months [33]. Muhire et al. [26] reported increased aridity in the rainy season in Rwanda in the period 1961–1992, but a wet trend in other months. In summary, there has not been unanimous scientific agreement on the causes of spatiotemporal variation in aridity or moisture or on the causes of drier or wetter regional climates.

Studies have found that in China (1) both wet [1, 31, 34] and dry trends [6, 15, 21, 22] occurred in different regions and during different seasons; (2) the drivers of wet and dry trends were not only temperature and precipitation but also other meteorological parameters such as WS, SSH, and RH [6, 7, 15, 21, 31, 32, 34]; and (3) most research was concerned with arid areas of northern and western China but ignored wet and dry trends in the climate of humid southeastern China, which was greatly affected by global climate change due to human activity.

We conducted our research on Jiangsu province and proposed the hypothesis that increasing air temperature, mainly induced by global warming and rapid regional urbanization, would lead to a dry trend in this province. The aims of this study were (1) to explore the spatiotemporal changes that determine the humidity index using the observed meteorological data; (2) to determine the contribution of each meteorological parameter to variation in the humidity index; and (3) to perform sensitivity analysis to identify the relative change in HI due to relative changes in the five parameters T_a, WS, RH, SSH, and Pre.

2. Study Area

Jiangsu province (30°45′–35°20′N, 116°18′–121°57′E) is an important economic and agricultural region in southeastern China. It has a high population density of 770 people/km^2 [35, 36] and has witnessed the most rapid urbanization in China [36]. Intensification of human activities, land use changes associated with urbanization, increased industrial emissions, and a sharp increase in water demand have influenced its regional climate and thus affected dry-wet climate trends as well as the forces of global climate change. The province is surrounded by Zhejiang province and the city of Shanghai to the south, Anhui province in the west, Shandong province in the north, and the Yellow Sea in the east; the coastline is over 1000 km long (Figure 1). Jiangsu province is 460 km from north to south and is partitioned into three regions (Huaibei, Jianghuai, and Sunan) by the Huai River and the Yangtze River (Figure 1). The province spans more than 5° of latitude, which leads to differences in the regional climate of three regions, such as an air temperature range of 13–16.5°C and a precipitation range of 800–1200 mm [37]. These differences in regional climate cause differences in moisture between the regions. We therefore examined the moisture in each region as well as in the province as a whole.

3. Materials and Methods

3.1. Data Source. Meteorological data used in the study included daily mean air temperature (T_a, °C), maximum temperature (T_{max}, °C), minimum temperature (T_{min}, °C), wind speed (WS, m/s), sunshine hours (SSH, h), relative humidity (RH, %), and precipitation (Pre, mm) measured at 24 stations during 1960–2019. All data were preprocessed by the China Meteorology Administration according to the 2004 *Standard of Surface Meteorology Observation by the China Meteorology Administration* was shared in the China Meteorological Data Service Center (http://data.cma.cn/).

Jiangsu province has been an important rice-growing region for thousands of years [38]. We conducted our research for individual seasons, spring (March–May), summer (June–August), autumn (September–November), and winter (December–February in the next year) as well as the entire year (January–December) and the rice-growing season (May–October).

3.2. Humidity Index. The humidity index HI is calculated by [39]

$$\mathrm{HI} = \frac{P}{\mathrm{ET}_o}, \tag{1}$$

where P is precipitation (mm) and ET_o is reference evapotranspiration (mm) and was calculated by the FAO 56 Penman–Monteith (PM) model. This model has been recommended by the Food and Agricultural Organization (FAO) and is expressed as [40]

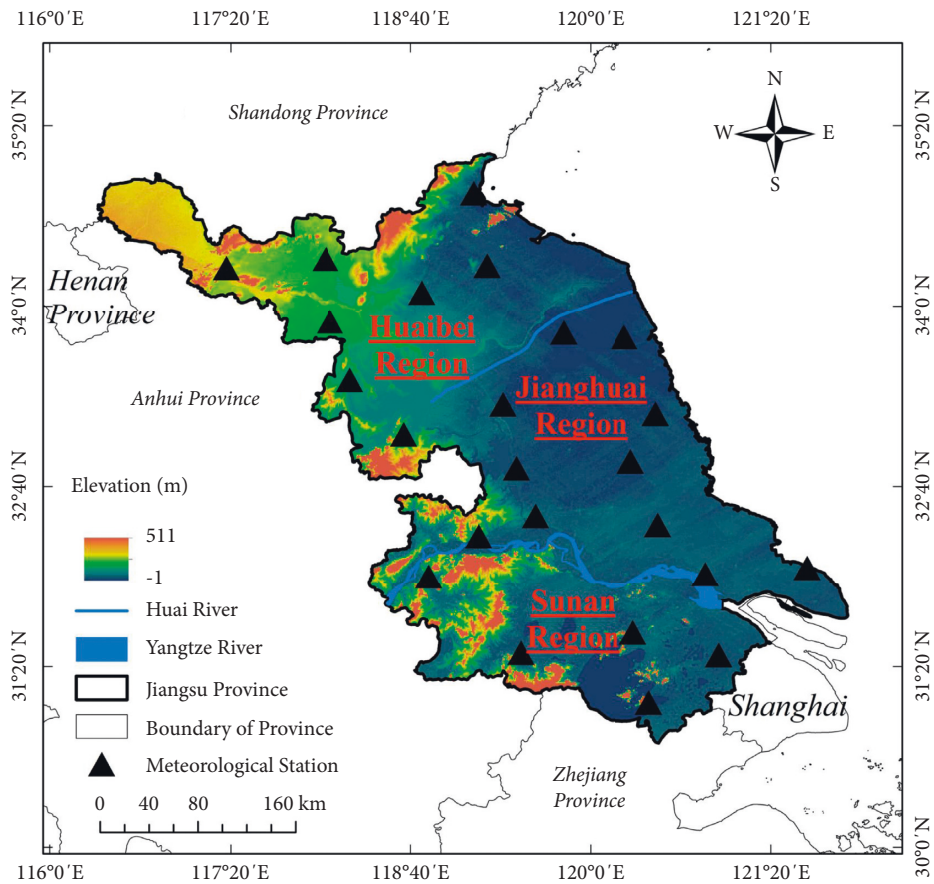

Figure 1: The three regions of Jiangsu province (Huaibei, Jianghuai, and Sunan), rivers, and meteorological stations.

$$\mathrm{ET}_o = \frac{0.408\Delta(R_n - G) + \gamma(900/T + 273)U_2(e_s - e_a)}{\Delta + \gamma(1 + 0.34U_2)}, \quad (2)$$

where R_n is the net radiation at the crop surface (MJ/m^2/d); G is the soil heat flux density (MJ/m^2/d), which can be ignored at a daily scale; T is the mean daily air temperature (°C); U_2 is the wind speed at 2 m height (m/s); e_s is the saturation vapor pressure (kPa); e_a is the actual vapor pressure (kPa); γ is the psychrometric constant (kPa/oC); and Δ is the slope of the vapor pressure curve (kPa/oC).

A set of equations were devised by Allen et al. [40] to calculate the parameters in equation (2), which we used with the daily meteorological data of 24 stations in Jiangsu province. We calculated $\mathrm{ET_o}$ at a daily scale using equation (2), combined observed daily precipitation data with calculated daily $\mathrm{ET_o}$ at seasonal and annual scales, and then used equation (1) to compute seasonal and annual HI for each region and for the entire province.

3.3. Trend Analysis. The trend of long-term climatic data is a critical indicator in analyzing climate change. Many kinds of trends can be defined, such as extrinsic and predetermined trends, intrinsic and adaptive trends, and using empirical mode decomposition for trend extraction [41]. The commonest and most simple trend is a straight line fitted to the data. A trend can be found by identifying changes in the moving average of a data series. In addition to these, trends that emerge from complicated trend extraction methods (such as regression analysis and Fourier-based filtering) are all extrinsic and predetermined trends. In this study, we used linear fitting and the Mann–Kendall test to identify extrinsic predetermined trends [42, 43] to identify changes in meteorological parameters and HI at both seasonal and annual scales. The Mann–Kendall test was also used to determine the significance of the trends at the 0.001, 0.01, 0.05, or 0.1 levels. The Mann–Kendall test is based on the hypothesis that the expected change in the series is a monotonic trend. The null hypothesis H_0 is that in a data series X (X_k, $k = 1, 2, \ldots, n$), X_k is independent and randomly distributed. The alternative hypothesis H_1 is that a monotonic trend exists in X. The statistic S is calculated as

$$S = \sum_{k=1}^{n-1} \sum_{j=k+1}^{n} \mathrm{sgn}(X_j - X_k), \quad (3)$$

where X_j represents the sequential data values, n is the number of the dataset, and

$$\mathrm{sgn}(X_j - X_k) = \begin{cases} 1, & \text{if } X_j - X_k > 0, \\ 0, & \text{if } X_j - X_k = 0, \\ -1, & \text{if } X_j - X_k < 0. \end{cases} \quad (4)$$

When $n > 10$, S is approximately normally distributed with $E(S) = 0$. The variance of statistic S can be calculated by

$$\mathrm{Var}(S) = \frac{1}{18}\left[n(n-1)(2n+5) - \sum_{w=1}^{v} t_p(t_w - 1)(2t_w + 5)\right], \tag{5}$$

where v is the number of tied groups and t_w is the number of data values in group w.

The standard test statistic (Z) is

$$Z = \begin{cases} \dfrac{s-1}{\sqrt{\mathrm{Var}(s)}}, & \text{if } s > 0, \\ 0, & \text{if } s = 0, \\ \dfrac{s+1}{\sqrt{\mathrm{Var}(s)}}, & \text{if } s < 0. \end{cases} \tag{6}$$

The null hypothesis H_0 is rejected when $|Z| > Z_{1-\alpha/2}$, where $Z_{1-\alpha/2}$ is the standard normal deviation. $|Z| > 1.28$, 1.64, and 2.32 indicate that change trends are significant at > 90% ($p < 0.1$), >95% ($p < 0.05$), and >99% ($p < 0.01$), respectively.

The Theil–Sen estimator [44, 45] was used to evaluate the magnitudes of the parameter trends. These simple but effective statistical methods have been widely used in hydrological-meteorological time series dataset trend analysis [32, 46–49]. The Theil–Sen estimator is calculated as

$$\beta = \mathrm{Median}\left(\frac{X_j - X_k}{j-k}\right), \quad 1 < k < j < n, \tag{7}$$

where β is the estimated magnitude of the slopes of HI trends. $\beta > 0$ represents an increasing trend, and $\beta < 0$ represents a decreasing trend.

3.4. Detrended Method. Linear detrending was used to quantify the contributions of five meteorological variables to the trend of HI at both seasonal and annual scales for each region and for the entire Jiangsu province. Previous studies [50–55] have described this method in three steps. (1) For each meteorological parameter, detrend the parameter time series to remove any overall increasing or decreasing trend. (2) Recalculate HI using one detrended meteorological parameter time series with the other four original parameter time series, and repeat this for each parameter. (3) Compare the recalculated HI with the original HI and use the indicator R to quantify the changes in meteorological variables that affect the trends in HI. R is calculated by

$$R = \sum_{i=1}^{m} \frac{\left(\mathrm{HI}_o^o - \mathrm{HI}_o^R\right)}{\mathrm{HI}_o^o i}, \tag{8}$$

where HI_o^o and HI_o^R are the original and the recalculated HI, respectively, and m is the length of the time series. $R > 0$, $R < 0$, and $R = 0$ indicate the positive, negative, and null effects of changes in the parameter on HI. A greater value of $|R|$ indicates a greater contribution of this variable to the HI trend.

3.5. Sensitivity Analysis. We used the method of sensitivity analysis developed by McCuen et al. [56] to identify the percentage change in HI due to percentage change in each meteorological parameter. This method has been widely used to analyze the sensitivity coefficients that relate ET_o to various meteorological parameters [57–60], and the method has also been used in recent years to examine the sensitivity of the dry-wet index to meteorological parameters [31, 61–63]. The sensitivity coefficient of HI to a meteorological parameter is calculated by

$$S_{xi} = \lim_{\Delta x_i \longrightarrow 0}\left(\frac{\Delta \mathrm{HI}/\mathrm{HI}}{\Delta x_i / x_i}\right) = \frac{\partial \mathrm{HI}}{\partial x_i}\frac{x_i}{\mathrm{HI}}, \tag{9}$$

where x_i is meteorological parameter i, and $S(x_i)$ is the sensitivity coefficient of the parameter and indicates the percentage change in HI caused by a percentage change in the parameter x_i. A positive or negative value of $S(x_i)$ indicates whether HI will increase or decrease as the parameter x_i increases.

4. Results

4.1. Temporal Variation of Five Meteorological Variables and Reference Evapotranspiration (ET_o). T_a has shown significant increasing trends ($p < 0.05$) in Jiangsu province over the past 60 years, with lower and similar rates of change in Huaibei and Jianghuai (Table 1). T_a in southern Sunan had the greatest rate of increase, and T_a increased for the entire province at respective rates of 0.041, 0.015, 0.026, 0.036, 0.022, and 0.29°C/y for spring, summer, fall, winter, growing season, and annually (Table 1). The rates of change of T_a were ordered as spring > winter > annual > autumn > growing season > summer (Table 1).

In contrast to T_a, WS for the three regions and the entire province showed significant decreasing trends ($p < 0.05$) over the period 1960–2019 (Table 1). One notable difference from the behavior of T_a was that the greatest variation in WS was found in northern Huaibei with a decreasing rate of change ranging from −0.027 m/s/y in spring to −0.02 m/s/y in autumn (Table 1). The rates of change in WS in Jianghuai and Sunan were both less than that in northern Huaibei and resulted in the decreasing trends ranged from −0.022 m/s/y in spring to −0.015 m/s/y in summer for the entire province (Table 1).

In the period 1960–2019, RH also showed decreasing trends in Jiangsu province (Table 1). The negative rates of change in RH were least in Huaibei, in the range of −0.106%/y ($p < 0.05$) in spring to −0.013%/y in winter. In southern Sunan, RH had the greatest rate of decrease, between −0.223%/y ($p < 0.001$) in spring and −0.076%/y ($p < 0.05$) in winter (Table 1). RH for the entire province decreased significantly ($p < 0.01$) in all seasons except for winter, when RH decreased at an insignificant rate −0.047%/y. The significantly decreasing trends of the entire province ranged from −0.161%/y in spring to −0.078%/y in both summer and autumn (Table 1).

There was little change in SSH in spring for all three regions during 1960–2019 (Table 1). In the other three seasons and annually, SSH showed significant decreasing trends ($p < 0.05$) for the three regions (Table 1). Similar to

Table 1: Seasonal and annual trends of daily mean air temperature (T_a), wind speed (WS), relative humidity (RH), sunshine hours (SSH), precipitation (Pre), and reference evaporation (ET_o) in Huaibei (HB), Jianghuai (JH), Sunan (SN), and the entire Jiangsu province during 1960–2019 using the Mann–Kendall and Theil–Sen estimator tests.

Variable	Zone	Spring	Summer	Autumn	Winter	Growing season	Annual
T_a (°C/y)	HB	0.039***	0.011*	0.023***	0.04***	0.019***	0.028***
	JH	0.038***	0.013*	0.024***	0.036***	0.02***	0.027***
	SN	0.049***	0.022**	0.035***	0.048***	0.03***	0.037***
	Whole	0.041***	0.015*	0.026***	0.036***	0.022***	0.029***
WS (m/s/y)	HB	−0.027***	−0.021***	−0.02***	−0.022***	−0.021***	−0.023***
	JH	−0.021***	−0.013***	−0.016***	−0.019***	−0.014***	−0.017***
	SN	−0.019***	−0.014***	−0.015***	−0.022***	−0.014***	−0.017***
	Whole	−0.022***	−0.015***	−0.017***	−0.021***	−0.016***	−0.019***
RH (%/y)	HB	−0.106*	−0.035+	−0.046	−0.013	−0.035*	−0.044*
	JH	−0.164***	−0.077**	−0.073+	−0.049***	−0.088***	−0.089***
	SN	−0.223***	−0.121***	−0.139***	−0.076*	−0.159***	−0.135***
	Whole	−0.161***	−0.078***	−0.078**	−0.047	−0.09***	−0.084***
SSH (h/y)	HB	−0.007	−0.036***	−0.021***	−0.027***	−0.028***	−0.023***
	JH	0.005	−0.031***	−0.013*	−0.017***	−0.02***	−0.015***
	SN	0.005	−0.036***	−0.015**	−0.02**	−0.023***	−0.018***
	Whole	0.003	−0.033***	−0.015**	−0.02***	−0.024***	−0.018***
Pre (mm/y)	HB	−0.33	−1.2*	−0.17	0.64**	−1.78*	−1.55*
	JH	−0.53	0.55	0.13	1.02**	0.06	0.59
	SN	−0.52	1.84*	0.19	1.7***	1.68*	2.8*
	Whole	−0.45	0.44	0.09	1.07***	0.23	0.53
ET_o (mm/y)	HB	0.04	−0.82***	−0.28*	−0.19*	−0.19***	−1.37***
	JH	0.65***	−0.25	0.06	−0.01	0.003	0.33
	SN	1.04***	−0.02	0.36**	0.01	0.75*	1.32**
	Whole	0.56**	−0.38*	0.01	−0.04	−0.14	0.05

Note: ***, **, *, and + indicate significance levels of 0.001, 0.01, 0.05, and 0.1, respectively.

WS, these SSH trends were the greatest in northern Huaibei and were least in Jianghuai and Sunan; rates of decrease were between −0.036 h/y in summer for Huaibei and −0.013 h/y in autumn for Jianghuai (Table 1). For the entire province, SSH showed a significant decreasing trend ($p < 0.01$) for three seasons (there was almost no change in spring) and annually. The negative rates of change ranged from −0.033 h/y in summer to −0.015 h/y in autumn (Table 1).

Table 1 shows that in the period 1960–2019, Pre showed a significant positive increasing trend ($p < 0.01$) in winter with a rate of change of 0.64 mm/y in Huaibei. However, Pre decreased significantly in Huaibei at a rate of −1.2 mm/y ($p < 0.05$) in summer and showed significant decreasing trends ($p < 0.05$) in the growing season (−1.78 mm/y) and annually (−1.55 mm/y) (Table 1). In southern Sunan, Pre increased significantly ($p < 0.05$) in summer and winter and annually with rates of change between 1.68 mm/y for the growing season and 2.8 mm/y at the annual scale; changes for spring and autumn were not significant (Table 1). Pre showed significant ($p < 0.01$) increasing trends, with rates of change of 1.02 and 1.07 mm/y, for Jianghuai and the entire province only for winter (Table 1), respectively.

Similar to Pre, ET_o showed both positive and negative trends for different seasons and annually in each region and the entire province (Table 1). In northern Huaibei, this variable showed significant decreasing trends ($p < 0.05$) in all seasons except spring, with little change (Table 1). The negative rates of change in Huaibei ranged from −0.082 mm/y for summer to −0.019 mm/y for both winter and the growing season. Jianghuai differed from Huaibei, showing significant changes in ET_o only for spring ($p < 0.001$) with a rate of change of 0.65 mm/y (Table 1). Southern Sunan showed significant increasing trends ($p < 0.01$) for spring and winter with rates of change of 1.04 and 0.36 mm/y, which resulted in ET_o increasing significantly ($p < 0.05$) by 0.75 and 1.32 mm/y, respectively, in the growing season and annually (Table 1). The changes in seasonal and annual ET_o in each region eventually caused ET_o for the entire province to increase in spring and autumn and annually and decrease in the other seasons. However, these changes were only significant in spring and summer, with rates of change of 0.56 and −0.38 mm/y (Table 1).

4.2. Analysis of Seasonal and Annual Humidity Index (HI)

4.2.1. Characteristics of Monthly Humidity Index (HI), Reference Evapotranspiration (ET_o), and Precipitation (Pre). Variations in monthly Pre, ET_o, and HI are shown in Figure 2. It is clear that both Pre and ET_o first increased and then decreased, with maximum values of 233 and 137 mm in July. These two variables had minimum values of almost 25 mm for winter (December–February). Maximum HI was 1.7, also for July, with the greatest positive difference between Pre and ET_o. The greatest negative difference between Pre and ET_o was for May, with minimum HI close to 0.7.

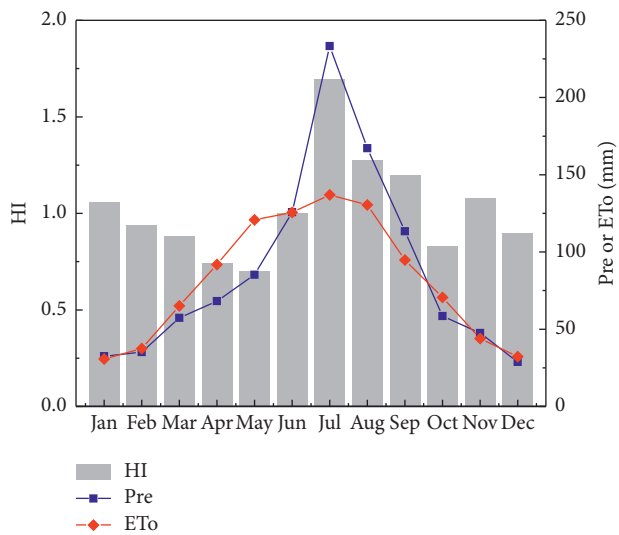

Figure 2: Variations in monthly humidity index (HI), reference evapotranspiration (ET_o), and precipitation (Pre).

4.2.2. Spatiotemporal Characteristics of Seasonal and Annual Humidity Index (HI) in Jiangsu Province. During 1961–2019, the increasing HI was only found in two sites of the Huaibei region in spring. For the other two regions in this season, we observed decreasing HI in all 17 sites (Figure 3(a)). In summer, the HI increased in 57.1%, 83.3%, and 100% of the sites of Huaibei, Jianghuai, and Sunan regions, respectively (Figure 3(b)).

In autumn, the HI generally showed increasing trends in Huaibei and Jianghuai regions with 85.7% and 58.3% of the sites with positive trends in each region (Figure 3(c)), respectively. For the southern Sunan region, the decreasing HI was found in all sites during 1961–2019 (Figure 3(c)). It was observed that the HI showed increasing trends in winter in all sites of Jiangsu province (Figure 3(d)). The decreasing HI was observed in 71.4% of the sites of the Huaibei region in both the growing season and annually (Figures 3(e) and 3(f)). Also, in these two periods, the HI showed increasing trends in most sites of the Jianghuai region (66.6% for the growing season and 75% annually) in 1961–2019. Furthermore, the increasing HI was found in all sites of the southern Sunan region in the growing season and annually (Figures 3(e) and 3(f)).

In addition to each site, we also used the Mann–Kendall test to examine seasonal and annual trends of HI in the whole Huaibei and Jianghuai Sunan regions, and Jiangsu province (Table 2), which were generally consistent with those shown in Figure 3. The Mann–Kendall test showed increasing trends in summer (only significant in Sunan) and winter (significant in all three regions and the entire province) during 1960–2019. In spring, the HI decreased in all three regions and the entire Jiangsu province but the decrease was only significant in Jianghuai and Sunan regions (Table 2). In autumn, the HI showed insignificant positive trends in Huaibei and Jianghuai regions and insignificant negative trends in Sunan and the entire province. Table 2 also exhibits that the growing season and annual HI only decreased in the Huaibei region and showed increasing trends in the other two regions and the entire province.

4.3. Sensitivity of Humidity Index (HI) to Key Meteorological Variables. Figure 4 shows the sensitivity coefficients relating HI to the five meteorological variables in each region and the entire province at both seasonal and annual scales for the period 1960–2019. The HI in Jiangsu province was clearly negatively sensitive to T_a, WS, and SSH, and positively sensitive to RH and Pre (Figure 4). The HI was least sensitive to T_a in winter; the absolute values of the sensitivity coefficients were <0.1 for all three regions and the entire province (Figure 4(a)). The HI was more sensitive to T_a in the other seasons and annually, with sensitivity coefficients ranging from −0.5 for Huaibei in spring to −0.23 for Sunan in autumn (Figure 4(b)). The HI was most sensitive to WS in Jiangsu province in winter and showed less sensitivity in the other seasons and annually (Figure 4(b)). The sensitivity coefficients were less than for T_a and ranged between −0.015 for Huaibei in summer and −0.02 for Sunan in winter (Figure 4(b)). The HI was more sensitive to SSH than to T_a and WS in Jiangsu province (Figure 4(c)). The HI was least sensitive to SSH in winter; sensitivity coefficients ranged from −0.33 in Huaibei to −0.18 in Sunan. For other seasons and annually, the absolute values of sensitivity coefficients of SSH were all >0.3, with maximum values in Huaibei −0.97 in spring, −0.93 in summer, −0.92 in the growing season, and −0.69 both in autumn and annually (Figure 3(c)).

The HI in Jiangsu province was positively sensitive to RH and Pre. It can be seen that the sensitivity of HI to RH was small to negligible, being <0.05 (Figure 4(d)). HI showed the greatest sensitivity to Pre in each region and the entire province, with sensitivity coefficients all >1 (Figure 4(e)). The sensitivity of HI to Pre at an annual scale was the greatest, with coefficients ranging from 1.47 in Jianghuai to 1.52 in Sunan. The sensitivity of HI to Pre was least in summer, with coefficients in the range of 1.09 in Sunan to —1.13 in Jianghuai (Figure 4(e)).

In Jiangsu province, the HI was most sensitive to Pre, followed by SSH, T_a, WS, and RH, in all seasons and annually except for winter (Figure 4). In the cold and dry winter, the sensitivity of HI to all five meteorological parameters was ranked Pre > SSH > WS > T_a > RH (Figure 4).

4.4. Contributions of Five Key Meteorological Parameters to Humidity Index (HI) Trends. We used the indicator R_{HI}, calculated by linear detrending, to evaluate the effects of changes in each meteorological variable on HI trends for different seasons and different regions (Figure 5). In spring, the decreases in RH and Pre were the main reasons for decreases in HI in all regions and the entire province. RH contributed more in Sunan (Figure 5(c)), and Pre contributed more in the other regions and the entire province (Figure 5(a), 5(b), and 5(d)). In summer, the negative effects of the decrease in Pre countered the positive effects of the changes in SSH and WS, resulting in little change in HI in Huaibei (Figure 5(a)). For the other two regions and the entire province, the HI increases in summer were mainly

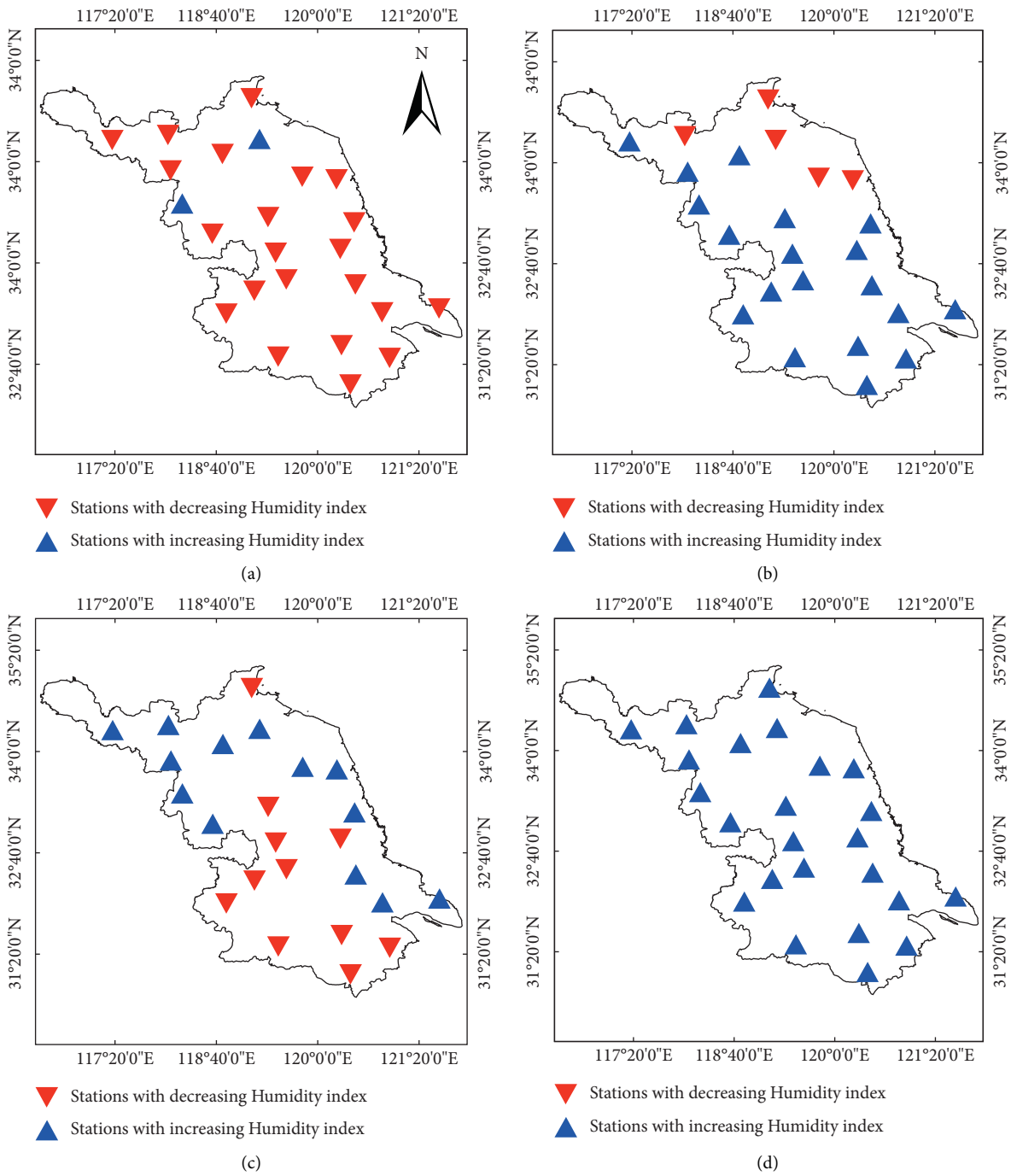

Figure 3: Continued.

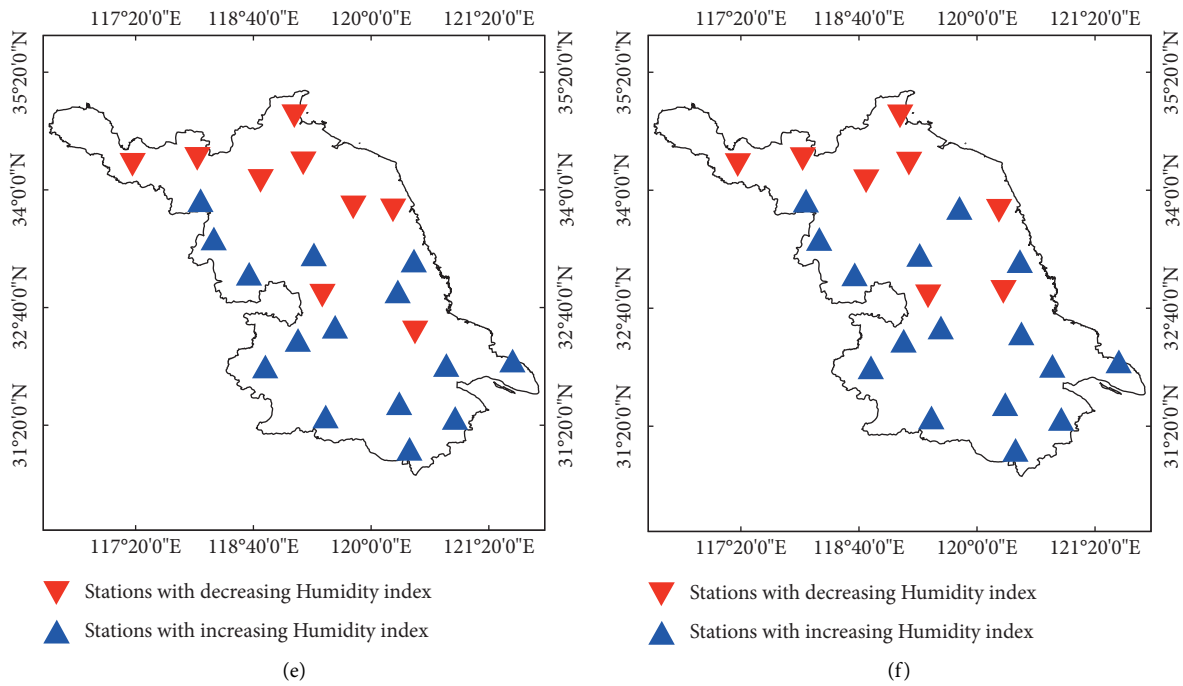

Figure 3: Spatial distribution of the sites with decreasing or increasing humidity index (HI) at seasonal and annual scales during 1961–2019 throughout Jiangsu province; the solid red inverted and blue regular triangles indicate the negative and positive trends of HI, respectively. (a) Spring, (b) summer, (c) autumn, (d) winter, (e) growing season, (f) annual.

Table 2: Trends of seasonal and annual humidity index (HI) in Huaibei, Jianghuai, Sunan, and the entire province during 1960–2019 using the Mann–Kendall test.

Season	Huaibei	Jianghuai	Sunan	Entire province
Spring	↓	↓$^{+}$	↓*	↓
Summer	↑	↑	↑$^{+}$	↑
Autumn	↑	↑	↓	↓
Winter	↑**	↑**	↑***	↑**
Growing season	↓	↑	↑	↑
Annual	↓	↑	↑	↑

Note: ***, **, *, and $^{+}$ indicate significance levels of 0.001, 0.01, 0.05, and 0.1, respectively.

caused by changes in WS, SSH, and Pre, with Pre having a greater effect than the other parameters in Sunan (Figure 5(c)), the decrease in SSH had a greater effect in both Jianghuai and the entire province (Figure 5(b) and 5(d)).

In autumn, similar to spring, the decreases in RH and Pre had the most effect on the negative trend of HI in Huaibei (Figure 5(a)). However, the combined effects of different parameters caused insignificant changes in the HI in the other two regions and the entire province in autumn (Figure 5). It is clear that the significant increase in Pre was responsible for the positive HI in Jianghuai, Sunan, and the entire province in winter (Figures 5(b)–5(d)). In northern Huaibei in winter, the decrease in WS had the most influence on the increase in HI (Figure 5(a)). In the growing season May–October, the large negative effect of a decrease in Pre overwhelmed the positive effects of decreases in WS and SSH, which resulted in the slightly decreasing trend of HI in Huaibei (Figure 5(a)). Also in the growing season, Pre showed an increasing trend and was dominant in the increase in HI in southern Sunan (Figure 5(c)). For Jianghuai and the entire province, decreases in WS and SSH (especially in WS) were the main reasons for the increase in HI in the growing season (Figures 5(b) and 5(d)). At the annual scale, the effects of SHH, WS, and Pre offset each other and resulted in little change in HI in Huaibei (Figure 5(a)). Similar to the growing season, the increase in Pre dominated the positive trend of HI in Sunan (Figure 5(c)), and the decreases in WS and SSH together were mainly responsible for the increase in HI in both Jianghuai and the entire province (Figures 5(b) and 5(d)).

Decreases in Pre and RH in Jiangsu province were generally responsible for the negative trends of HI in spring and autumn; the positive trends of HI in summer and winter were mainly due to decreases in WS and SSH and increases in Pre (Figure 5). In the growing season and annually in Jianghuai, Sunan, and the entire province, the decreases in WS and SSH and increases in Pre were the main causes of the increase in HI. The slight decreasing trend in HI in the growing season and annually in northern Huaibei was mainly caused by the decrease in Pre which counterbalanced the positive effects of changes in WS and SSH (Figure 5).

5. Discussion

5.1. Dry and Wet Trends in Jiangsu Province. Similar to some previous studies in China [6, 21, 32, 33, 48, 64, 65]. We found that the climate of Jiangsu province also exhibited different dry-wet trends in different seasons and annually during 1960–2019 (Figure 3). We found a dry trend in Jiangsu

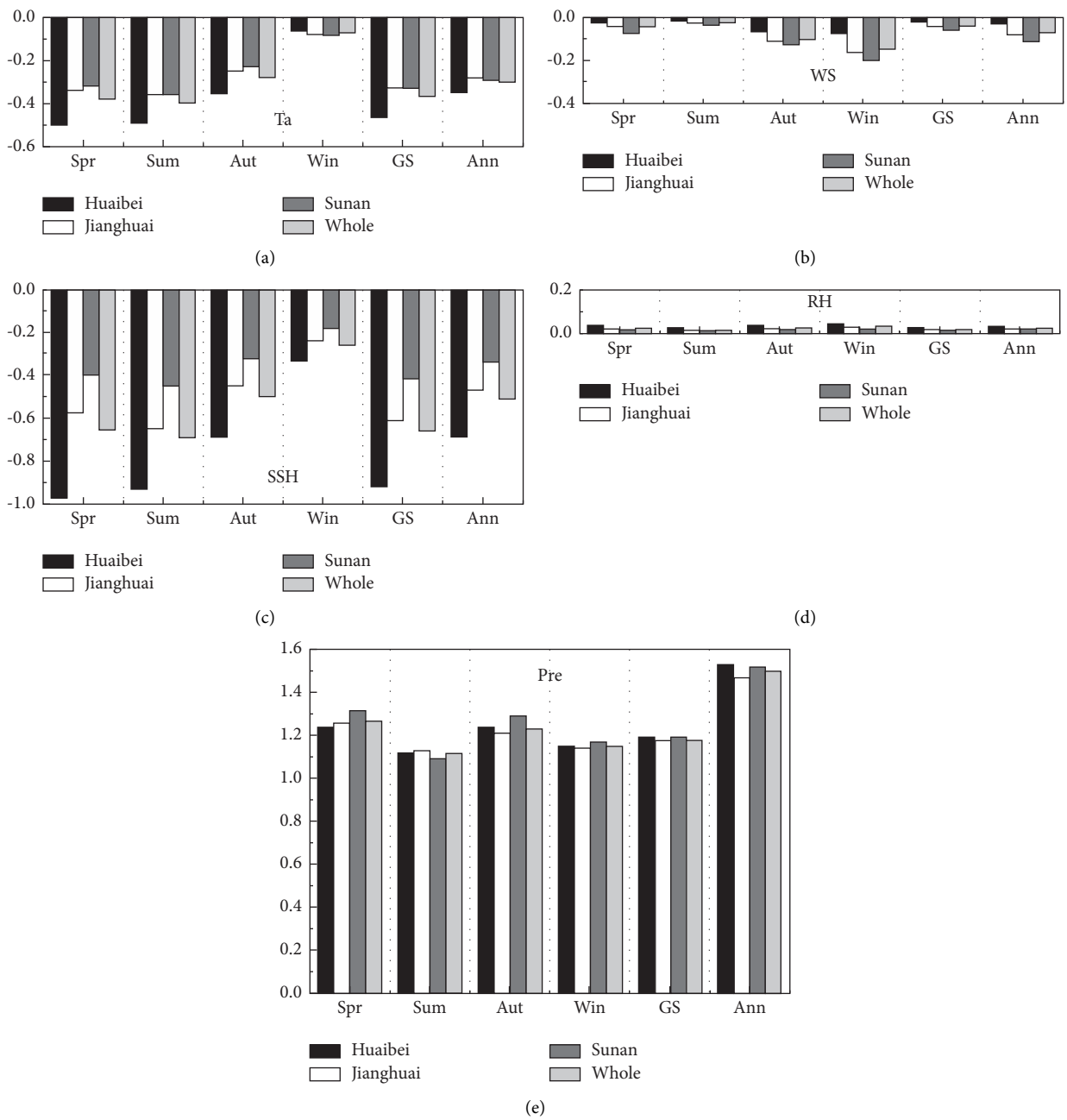

Figure 4: Sensitivity coefficients of seasonal and annual humidity index (HI) to five principal meteorological parameters in each region and the entire province; T_a, WS, SSH, RH, and Pre are mean daily air temperature, wind speed, sunshine hours, relative humidity, and precipitation, respectively.

Province in spring and autumn in the period 1960–2019 (Figures 3(a) and 3(c)). This was consistent with findings for some regions within China, such as the Zoige Wetland in southwestern China for 1961–2016 [21], Zhejiang province in southeastern China for 1961–2016 [33], Bosten Lake basin, and the Loess Plateau in northern China for 1980–2016 and 1961–2014 [15, 22]. Wang et al. [6] investigated dry-wet trends in China and found a drought tendency in the semi-arid or semi-humid and humid areas of southwestern China for a recent 58-year period. Wu et al. [7] found that the overall trend in China had changed from wet to dry since 1954. Worldwide, a drying climate has been observed in many countries, such as Finland [66], South Africa [67], Spain [17], India [27], Iraq [20], Iran [16], Rwanda [26], and Middle East and adjacent areas [28]. Except for spring and autumn, we detected a wet trend in Jiangsu province during 1960–2019 for the other seasons and annually (Figure 3). In reviewing previous studies, we noticed that areas with an increasingly wet climate were distributed mainly in western and northern China: Qinghai province [30], north Xinjiang [31], the Yellow River basin [49], and the Tibetan Plateau [15, 68]. Researchers have also

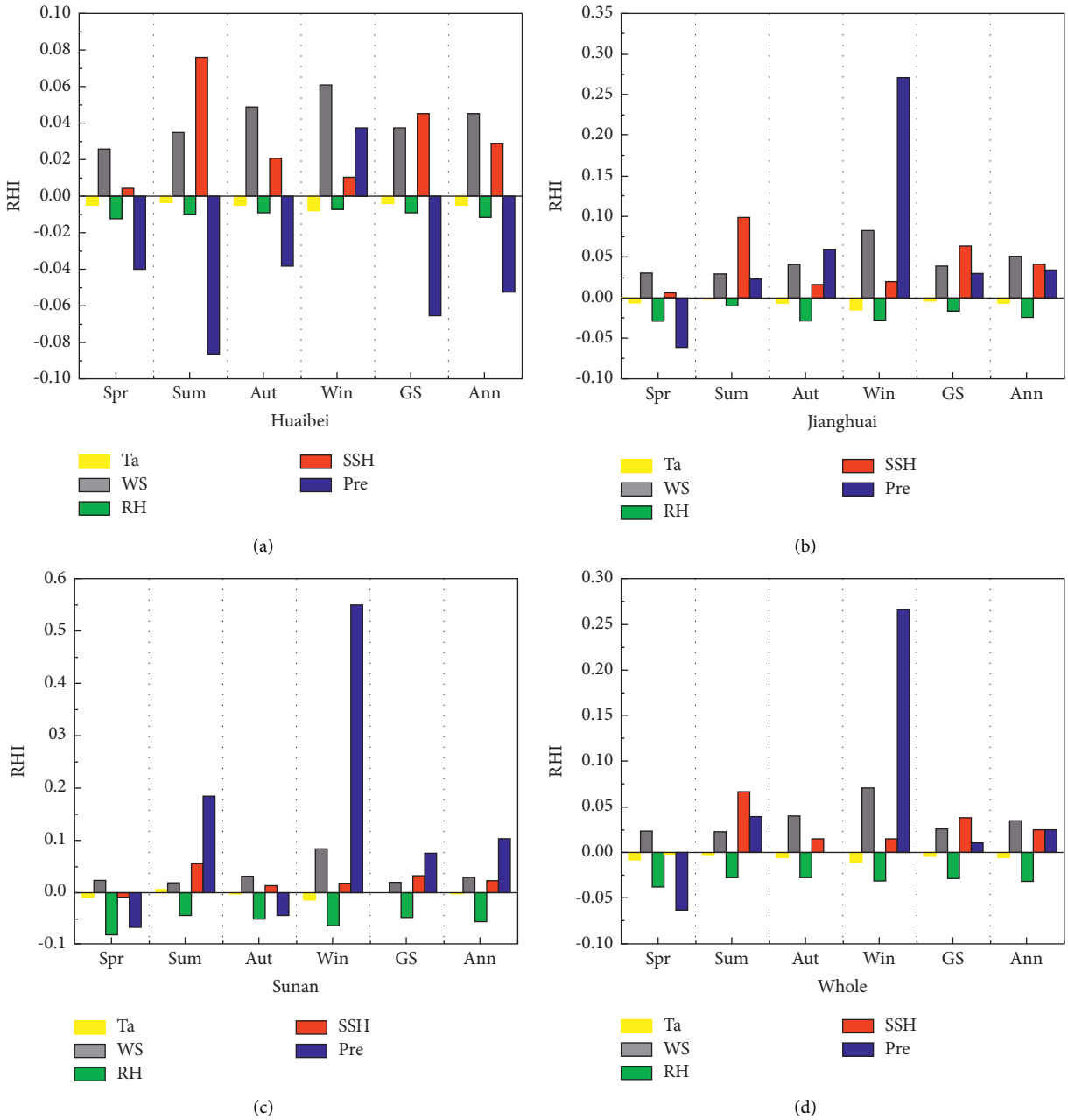

Figure 5: Contributions of five meteorological variables to humidity index (HI) trends at both seasonal and annual scales in (a) Huaibei, (b) Jianghuai, (c) Sunan, and (d) the entire province; T_a, WS, SSH, RH, and Pre are daily mean air temperature, wind speed, sunshine hours, relative humidity, and precipitation, respectively.

found an increasingly wet trend since 1970 for northwestern China and northern China west of longitude 100oE [34, 64]. However, the trend for an increasingly wet climate was found only for August in Zhejiang province in southeastern China for the period 1971–2015 and in summer, autumn, and annually for the humid regions of southern China for the period 1960–2017 [6, 33].

5.2. Contributions of Meteorological Variables to Humidity Index (HI) Trends. This study differs from most previous studies of trends of the humidity index, which considered only the effects of Pre, ET_o, and T_a [6, 7, 15, 20, 27–29, 48, 68]. We examined the effects of five meteorological variables, WS, RH, SSH, T_a, and Pre (Figure 5). We found that HI trends for each region and the entire province were primarily affected by changes in Pre in most seasons and annually during 1960–2019 (Figure 5). This result is consistent with the results of most previous studies [6, 7, 15, 20, 27, 32, 48]. However, for all three regions and the entire province, the decrease in RH had a negative effect on both seasonal and annual HI and was predominant in decreasing HI in spring for Sunan (Figure 5(c)). Changes in RH have been found to affect the humidity index in the Yellow River basin in

northern China [49] and the Zoige Wetland in southwestern China [21]. We also analyzed the effects of SSH and WS, which were included in only a few previous studies, and found that both contributed positively to the HI trend in Jiangsu province (Figure 5). Our previous study found that, for Jiangsu province in 1960–2019, the decrease in RH and SSH decreased ET_o [69], which increased HI.

5.3. Sensitivity of Humidity Index (HI) to Meteorological Variables. The HI was most sensitive to Pre in Jiangsu province for the period 1960–2019 (Figure 4(e)). This is consistent with results for both the entire northwestern and southwestern parts of China [34, 65]. Wang et al. [6] also found that dry-wet conditions were most sensitive to Pre in the humid regions of China that had annual precipitation >800 mm. Our results differ from previous studies, which found HI was secondarily sensitive to vapor pressure or ET_o [6, 34], as we found that in ranking parameters to which HI was sensitive, SSH ranked second (Figure 4(c)). This difference may be due to the exclusion of SSH from sensitivity analysis in previous studies [6, 34]. However, measured SSH indicated that a limited amount of energy was available at the surface [40, 51, 70] and it was therefore necessary to include it in the sensitivity analysis. The sensitivity of HI to T_a and WS was much less than to Pre and SSH, with absolute values of sensitivity coefficients in Jiangsu province all <0.5 (Figures 4(a), 4(b), and 4(d)). HI in the Gansu province of northwestern China showed the least sensitivity to WS and to minimum air temperature [63]. Liu et al. [34] also found that HI for northwest China in 1960–2010 was least sensitive to T_a and WS. Studies that include sensitivity analysis have mostly concentrated on arid areas within northern China, and further similar work must be conducted for humid southern China, which has experienced a dry trend [6, 32, 33].

5.4. Uncertainties and Future Research. In this research, we adopted the FAO 56 PM method to estimate ET_o and many mathematical methods to determine the dominant meteorological variable. However, the selected five meteorological variables were not totally independent, and the influences between them would impact the determination of dominant factors [34]. Another uncertainty was caused by these mathematical methods without considering the physical mechanism. These uncertainties forced researchers to search a hydrometeorological model, which can clarify the interaction between different meteorological variables with the help of underlying climatic mechanisms. Moreover, our research was conducted in Jiangsu province on the southeast coast of China. This is helpful to explore the dry-wet trends for the whole country by combining with the existing research in arid areas of northwest China. In addition to this, future research is still needed to focus on the potential impacts of dry-wet changes on human society.

6. Conclusion

We investigated the contributions of five meteorological variables (T_a, WS, RH, SSH, and Pre) to both seasonal and annual HI trends for three regions of Jiangsu province and the province as a whole in humid southeastern China for the 60-year period 1960–2019. The results showed the following: (1) the decreased Pre and RH were generally responsible for the negative trends of HI in spring and autumn. (2) The wet trend in summer and winter was mainly caused by decreases in WS and SSH and increases in Pre (Figure 5). (3) For the growing season and annually, the decreased WS and SSH and increased Pre were the main causes for positive HI in Jianghuai, Sunan, and the entire province. The slight decreasing HI in the growing season and annually in northern Huaibei was mainly caused by the decrease in Pre (Figure 5). Sensitivity analysis indicated that the HI in Jiangsu province was positively sensitive to Pre and RH and negatively sensitive to T_a, WS, and SSH over the 60-year period (Figure 4). The climate of Jiangsu province was most sensitive to changes in Pre and then, in the decreasing order of sensitivity, to SSH, T_a, WS, and RH in all seasons (except for winter) and annually. For winter, sensitivity was ranked Pre > SSH > WS > T_a > RH (Figure 4).

This study has shown that the regional climate has experienced a dry trend in some seasons during the period 1960–2019 despite the humidity in southeastern China. This will draw attention to the evolution of dry-wet conditions in humid southeastern China rather than the arid regions in western China. Furthermore, in addition to the Pre that was directly related to dry-wet conditions, the other climatic factors also impacted the dry-wet conditions and need to be considered in humid regions. As an important agricultural area in China, the observed dry trend may threaten existing irrigation systems and the security of water resources, which in turn affects crop yield in Jiangsu province. The contribution of each meteorological variable to HI trends, and the sensitivity of HI to each variable, can provide a basis for structural adjustment of farming systems in Jiangsu province at different spatiotemporal scales. Further work should extend this research to the entire humid area of southwestern China and clarify the mechanisms that lead to different trends of humidity indexes in different regions or over different seasons.

Data Availability

The raw data are shared in the China Meteorological Data Service Center: http://data.cma.cn/.

Conflicts of Interest

The authors declare that there are no conflicts of interest regarding the publication of this article.

Acknowledgments

This study was financially supported by the National Natural Science Foundation of China (Grant no. 42075051), Drought Meteorological Science Research Fund (Grant no. IAM202108), and Jiangsu Meteorological Bureau Science Foundation for Young Scholars (nos. KQ202126 and KQ202226).

References

[1] Y. Wang, Y. Xu, C. Lei et al., "Spatio-temporal characteristics of precipitation and dryness/wetness in Yangtze River Delta, eastern China, during 1960–2012," *Atmospheric Research*, vol. 172-173, pp. 196–205, 2016.

[2] N. Nicholls and L. Alexander, "Has the climate become more variable or extreme? Progress 1992-2006," *Progress in Physical Geography: Earth and Environment*, vol. 31, no. 1, pp. 77–87, 2007.

[3] M. A. Asadi Zarch, B. Sivakumar, and A. Sharma, "Droughts in a warming climate: a global assessment of standardized precipitation index (SPI) and reconnais-sance drought index (RDI)," *Journal of Hydrology*, vol. 526, pp. 183–195, 2015.

[4] S. M. Quiring and T. N. Papakryiakou, "An evaluation of agricultural drought indices for the Canadian prairies," *Agricultural and Forest Meteorology*, vol. 118, no. 1–2, pp. 49–62, 2003.

[5] A. K. Mishra and V. P. Singh, "Drought modeling—a review," *Journal of Hydrology*, vol. 403, no. 1–2, pp. 157–175, 2011.

[6] S. Wang, Q. Zhang, P. Yue, and J. S. Wang, "Effects of evapotranspiration and precipitation on dryness/wetness changes in China," *Theoretical and Applied Climatology*, vol. 142, no. 3-4, pp. 1027–1038, 2020.

[7] S. Wu and X. D. Yan, "Variations in droughts and wet spells and their influences in China: 1924–2013," *Theoretical and Applied Climatology*, vol. 135, no. 1-2, pp. 623–631, 2018.

[8] W. C. Palmer, *Meteorological Drought*, US Department of Commerce. US Weather Bureau, Washington, DC, USA, 1965.

[9] T. B. Mckee, N. J. Doesken, and J. Kleist, "The relationship of drought frequency and duration to time scales,"vol. 17, pp. 179–183, in *Proceedings of the 8th Conference on Applied Climatology*, vol. 17, pp. 179–183, American Meteorological Society, Boston, MA, USA, 1993.

[10] C. W. Thornthwaite, "An approach toward a rational classification of climate," *Geographical Review*, vol. 38, no. 1, pp. 55–94, 1948.

[11] S. M. Vicente-Serrano, S. Beguería, J. I. López-Moreno, M. Angulo, and A. El Kenawy, "A new global 0.5° gridded dataset (1901–2006) of a multiscalar drought index: comparison with current drought index datasets based on the palmer drought severity index," *Journal of Hydrometeorology*, vol. 11, no. 4, pp. 1033–1043, 2010.

[12] S. M. Vicente-Serrano, S. Beguería, J. I. Lorenzo-Lacruz et al., "Performance of drought indices for ecological, agricultural, and hydrological applications," *Earth Interactions*, vol. 16, no. 10, pp. 1–27, 2012.

[13] Q. Yang, M. X. Li, Z. Y. Zheng, and Z. G. Ma, "Regional applicability of seven meteorological drought indices in China," *Science China Earth Sciences*, vol. 47, no. 3, pp. 337–353, 2017.

[14] Z. G. Ma and C. B. Fu, "The basic facts of northern China from 1951 to 2004 drought," *Chinese Science Bulletin*, vol. 51, no. 20, pp. 2429–2439, 2006.

[15] M. Wen, D. Cheng, J. Song, G. Zhang, W. Lai, and W. Jiang, "Impacts of climate change on aridity index and its spatio-temporal variation in the Loess Plateau of China, from 1961 to 2014," *Environmental Earth Sciences*, vol. 77, no. 4, p. 137, 2018.

[16] H. Tabari and M. B. Aghajanloo, "Temporal pattern of aridity index in Iran with considering precipitation and evapotranspiration trends," *International Journal of Climatology*, vol. 33, no. 2, pp. 396–409, 2012.

[17] F. J. Moral, F. J. Rebollo, L. L. Paniagua, A. García-Martín, and F. Honorio, "Spatial distribution and comparison of aridity indices in extremadura, southwestern Spain," *Theoretical and Applied Climatology*, vol. 126, no. 3-4, pp. 801–814, 2016.

[18] Y. Wand, P. X. Liu, L. G. Cao, Y. Gao, and G. Z. Yong, "Characteristics of southwestern China dry-wet condition based on wetness index in 1960-2011," *Natural Resources Journal*, vol. 5, pp. 830–838, 2014.

[19] Y. F. Liu, Z. H. Yuan, J. M. Feng, L. Zhang, and L. Wu, "Dry-wet condition of shaanxi province in recent 56 Years based on surface humidity index," *Arid Land Geography*, vol. 39, no. 6, pp. 1186–1196, 2016.

[20] N. Şarlak and O. M. A. Mahmood Agha, "Spatial and temporal variations of aridity indices in Iraq," *Theoretical and Applied Climatology*, vol. 133, no. 1-2, pp. 89–99, 2018.

[21] X. Jin, H. Qiang, L. Zhao et al., "Spei-based analysis of spatio-temporal variation characteristics for annual and seasonal drought in the Zoige Wetland, southwest China from 1961–2016," *Theoretical and Applied Climatology*, vol. 139, no. 1-2, pp. 711–725, 2020.

[22] H. Yang, J. Xu, Y. Chen et al., "Has the Bosten Lake basin been dry or wet during the climate transition in northwest China in the past 30 years?" *Theoretical and Applied Climatology*, vol. 141, no. 1-2, pp. 627–644, 2020.

[23] Z. Zhang, Q. Zhang, X. Chen, J. Zhang, and J. Zhou, "Statistical properties of moisture transport in east asia and their impacts on wetness/dryness variations in north China," *Theoretical and Applied Climatology*, vol. 104, no. 3-4, pp. 337–347, 2011.

[24] S. K. MIn, W. T. Kwon, E. H. Park, and Y. Choi, "Spatial and temporal comparisons of droughts over Korea with east asia," *International Journal of Climatology*, vol. 23, no. 2, pp. 223–233, 2003.

[25] A. D. Mueller, G. A. Islebe, M. B. Hillesheim et al., "Climate drying and associated forest decline in the lowlands of northern Guatemala during the late holocene," *Quaternary Research*, vol. 71, no. 2, pp. 133–141, 2009.

[26] I. Muhire and F. Ahmed, "Spatiotemporal trends in mean temperatures and aridity index over Rwanda," *Theoretical and Applied Climatology*, vol. 123, no. 1-2, pp. 399–414, 2015.

[27] M. V. S. Ramarao, J. Sanjay, R. Krishnan, M. Mujumdar, A. Bazaz, and A. Revi, "On observed aridity changes over the semiarid regions of India in a warming climate," *Theoretical and Applied Climatology*, vol. 136, no. 1-2, pp. 693–702, 2018.

[28] H. Sahour, M. Vazifedan, and F. Alshehri, "Aridity trends in the Middle East and adjacent areas," *Theoretical and Applied Climatology*, vol. 142, no. 3-4, pp. 1039–1054, 2020.

[29] L. L. Paniagua, A. García-Martín, F. J. Moral, and F. J. Rebollo, "Aridity in the iberian Peninsula (1960–2017): distribution, tendencies, and changes," *Theoretical and Applied Climatology*, vol. 138, no. 1-2, pp. 811–830, 2019.

[30] Z. Liu, P. Zhou, F. Zhang, X. Liu, and G. Chen, "Spatio-temporal characteristics of dryness/wetness conditions across Qinghai province, northwest China," *Agricultural and Forest Meteorology*, vol. 182–183, pp. 101–108, 2013.

[31] Y. F. Wu, G. X. Zhang, H. Shen, Y. J. Xu, and B. Batur, "Attribute analysis of aridity variability in north Xinjiang, China," *Advances in Meteorology*, vol. 2016, Article ID 9610960, 11 pages, 2016.

[32] L. Liu, Y. Wang, N. You, Z. Liang, D. H. Qin, and S. Li, "Changes in aridity and its driving factors in China during 1961–2016," *International Journal of Climatology*, vol. 39, no. 1, pp. 50–60, 2019.

[33] W. Lou, L. Wu, Y. Mao, and K. Sun, "Precipitation and temperature trends and dryness/wetness pattern during 1971–2015 in Zhejiang province, southeastern China," *Theoretical and Applied Climatology*, vol. 133, no. 1-2, pp. 47–57, 2018.

[34] X. Liu, D. Zhang, Y. Luo, and C. Liu, "Spatial and temporal changes in aridity index in northwest China: 1960–2010," *Theoretical and Applied Climatology*, vol. 112, no. 1-2, pp. 307–316, 2013.

[35] L. Hao, X. Huang, M. S. Qin, Y. Q. Liu, W. H. Li, and G. Sun, "Ecohydrological processes explain urban dry island effects in a wet region, southern China," *Water Resources Research*, vol. 54, no. 9, pp. 6757–6771, 2018.

[36] C. Huang, M. Zhang, J. Zou et al., "Changes in land use, climate and the environment during a period of rapid economic development in Jiangsu province, China," *Science of the Total Environment*, vol. 536, pp. 173–181, 2015.

[37] M. Mai, S. P. Zha, and B. Zhu, "Agro-climatic resource zoning in Jiangsu province," *Meteorological and Environmental Research*, vol. 1, no. 11, pp. 59–63, 2010.

[38] L. Hao, G. Sun, Y. Q. Liu et al., "Urbanization dramatically altered the water balances of a paddy field-dominated basin in southern China," *Hydrology and Earth System Sciences*, vol. 19, no. 7, pp. 3319–3331, 2015.

[39] N. Pye, N. J. Middleton, and D. S. G. Thomas, "World atlas of desertification," *The Geographical Journal*, vol. 160, no. 2, p. 210, 1994.

[40] R. Allen, L. Pereira, D. Raes, M. Smith, and R. G. Allen, *Crop Evapotranspiration: Guidelines for Computing Crop Water Requirements*, Food and Agriculture Organization, Rome, Italy, 1998.

[41] Z. Wu, N. E. Huang, S. R. Long, and C. K. Peng, "On the trend, detrending, and variability of nonlinear and nonstationary time series," *Proceedings of the National Academy of Sciences of the United States of America*, vol. 104, no. 38, pp. 14889–14894, 2007.

[42] H. B. Mann, "Nonparametric tests against trend," *Econometrica*, vol. 13, no. 3, pp. 245–259, 1945.

[43] M. G. Kendall, "A new measure of rank correlation," *Biometrika*, vol. 30, no. 1-2, pp. 81–93, 1938.

[44] P. K. Sen, "Estimates of the regression coefficient based on kendall's tau," *Journal of the American Statistical Association*, vol. 63, no. 324, pp. 1379–1389, 1968.

[45] R. M. Hirsch, J. R. Slack, and R. A. Smith, "Techniques of trend analysis for monthly water quality data," *Water Resources Research*, vol. 18, no. 1, pp. 107–121, 1982.

[46] M. Nouri and M. Bannayan, "Spatiotemporal changes in aridity index and reference evapotranspiration over semi-arid and humid regions of Iran: trend, cause, and sensitivity analyses," *Theoretical and Applied Climatology*, vol. 136, no. 3-4, pp. 1073–1084, 2018.

[47] H. Ahani, M. Kherad, M. R. Kousari, L. van Roosmalen, R. Aryanfar, and S. M. Hosseini, "Non-parametric trend analysis of the aridity index for three large arid and semi-arid basins in Iran," *Theoretical and Applied Climatology*, vol. 112, no. 3-4, pp. 553–564, 2013.

[48] Y. Y. Zhou and C. X. Lu, "Drought/wetting variations in a semiarid and sub-humid region of China," *Theoretical and Applied Climatology*, vol. 140, no. 3-4, pp. 1537–1548, 2020.

[49] K. X. Zhang, S. M. Pan, W. Zhang et al., "Influence of climate change on reference evapotranspiration and aridity index and their temporal-spatial variations in the Yellow River basin, China, from 1961–2012," *Quaternary International*, vol. 380-381, pp. 75–82, 2015.

[50] C. Y. Xu, L. B. Gong, T. Jiang, D. L. Chen, and V. P. Singh, "Analysis of spatial distribution and temporal trend of reference evapotranspiration and Pan evaporation in changjiang (Yangtze River) catchment," *Journal of Hydrology*, vol. 327, no. 1–2, pp. 81–93, 2006.

[51] M. Qin, L. Hao, L. Sun, Y. Q. Liu, and G. Sun, "Climatic controls on watershed reference evapotranspiration varied during 1961–2012 in southern China," *JAWRA Journal of the American Water Resources Association*, vol. 55, no. 1, pp. 189–208, 2019.

[52] Q. Liu, Z. Yang, B. Cui, and T. Sun, "The temporal trends of reference evapotranspiration and its sensitivity to key meteorological variables in the Yellow River basin, China," *Hydrological Processes*, vol. 24, no. 15, pp. 2171–2181, 2010.

[53] Z. L. Huo, X. Q. Dai, S. Y. Feng, S. Z. Kang, and G. H. Huang, "Effect of climate change on reference evapotranspiration and aridity index in arid region of China," *Journal of Hydrology*, vol. 492, pp. 24–34, 2013.

[54] Z. J. Li, Z. Li, Z. Xu, and X. Zhou, "Temporal variations of reference evapotranspiration in heihe River basin of China," *Hydrology Research*, vol. 44, no. 5, pp. 904–916, 2013.

[55] M. Li, R. H. Chu, A. R. M. T. Islam, Y. Jiang, and S. S. Shen, "Attribution analysis of long-term trends of aridity index in the Huai River basin, eastern China," *Sustainability*, vol. 12, no. 5, p. 1743, 2020.

[56] R. H. Mccuen, "A sensitivity and error analysis of procedures used for estimating evaporation," *Journal of the American Water Resources Association*, vol. 10, no. 3, pp. 486–497, 1974.

[57] Y. H. Yin, S. H. Wu, and E. F. Dai, "Determining factors in potential evapotranspiration changes over China in the period 1971–2008," *Chinese Science Bulletin*, vol. 55, no. 29, pp. 3329–3337, 2010.

[58] L. Q. Liang, L. J. Li, and Q. Liu, "Temporal variation of reference evapotranspiration during 1961-2005 in the taoer River basin of northeast China," *Agricultural and Forest Meteorology*, vol. 150, no. 2, pp. 298–306, 2010.

[59] D. Zhang, X. M. Liu, and H. Y. Hong, "Assessing the effect of climate change on reference evapotranspiration in China," *Stochastic Environmental Research and Risk Assessment*, vol. 27, no. 8, pp. 1871–1881, 2013.

[60] Z. L. Wang, P. W. Xie, C. G. Lai et al., "Spatiotemporal variability of reference evapotranspiration and contributing climatic factors in China during 1961–2013," *Journal of Hydrology*, vol. 544, pp. 97–108, 2017.

[61] J. Du, D. Biao, J. Hu, B. La, and K. S. Zhou, "Responses of climatic change on surface humid index in northern tibet during the period of 1961–2006," *Acta Ecologica Sinca*, vol. 05, pp. 2437–2444, 2009.

[62] Y. Li, A. Feng, W. Liu, X. Ma, and G. Dong, "Variation of aridity index and the role of climate variables in the southwest China," *Water*, vol. 9, no. 10, p. 743, 2017.

[63] S. P. Wang, Y. H. Li, J. Y. Feng, J. S. Wang, and J. Wang, "Changes and driving factor of surface wetness in Gansu, China from 1961 to 2012," *Journal of Desert Research*, vol. 34, no. 6, pp. 1624–1632, 2014.

[64] K. Zhang, X. Qian, P. Liu et al., "Variation characteristics and influences of climate factors on aridity index and its association with ao and enso in northern China from 1961 to 2012," *Theoretical and Applied Climatology*, vol. 130, no. 1-2, pp. 523–533, 2017.

[65] Y. Zhao, X. Zou, L. Cao, Y. Yao, and G. Fu, "Spatiotemporal variations of potential evapotranspiration and aridity index in relation to influencing factors over southwest China during

1960–2013," *Theoretical and Applied Climatology*, vol. 133, no. 3-4, pp. 711–726, 2018.

[66] M. Irannezhad, A. Torabi Haghighi, D. Chen, and B. Kløve, "Variability in dryness and wetness in Central Finland and the role of teleconnection patterns," *Theoretical and Applied Climatology*, vol. 122, no. 3-4, pp. 471–486, 2015.

[67] M. Mbiriri, G. Mukwada, and D. Manatsa, "Spatiotemporal characteristics of severe dry and wet conditions in the free state province, South Africa," *Theoretical and Applied Climatology*, vol. 135, no. 1-2, pp. 693–706, 2018.

[68] Y. Zhao, X. Zou, J. Zhang et al., "Spatio-temporal variation of reference evapotranspiration and aridity index in the Loess Plateau region of China, during 1961–2012," *Quaternary International*, vol. 349, pp. 196–206, 2014.

[69] M. S. Qin, Y. Zhang, S. Q. Wan, Y. Yue, Y. Cheng, and B. Zhang, "Impact of climate change on "evaporation paradox" in province of Jiangsu in southeastern China," *PLoS One*, vol. 16, no. 2, Article ID e0247278, 2021.

[70] Z. D. Gao, J. S. He, K. B. Dong, and X. Li, "Trends in reference evapotranspiration and their causative factors in the west liao River basin, China," *Agricultural and Forest Meteorology*, vol. 232, pp. 106–117, 2017.